Proton Transfer

DOI: 10.1002/anie.200603583

Dynamic Protonation Equilibrium of Solvated Acetic Acid**

*Wei Gu, Tomaso Frigato, Tjerk P. Straatsma, and Volkhard Helms**

The biological functions of many proteins are crucially coupled to protonation equilibria, for instance, in the enzymatic reactions of serine proteases[1–3] and carbonic anhydrase,[4] and in integral membrane proton pumps such as bacteriorhodopsin,[5] cytochrome *c* oxidase (COX),[6,7] and F_OF_1-ATP synthase.[8] Proton-transfer (PT) reactions are also crucial in many other areas of chemistry, such as membrane permeation in hydrogen fuel cells and in polymers.[9] Despite their tremendous importance, many aspects of PT reactions in biomolecules remain poorly understood. As the direct observation of PT reactions by experimental techniques faces fundamental and/or technical difficulties, it is highly desirable to use computational methods as a complement.

In the past decades, various efficient computational methods have been developed to calculate the pK_a values of amino acid side chains as well as to perform simulations of proteins at constant pH,[10–17] using, for example, fractional charges[10] and implicit solvent models.[16,17] However, these methods do not model explicit proton-exchange reactions between the titratable sites and the surrounding aqueous solution or the exchange between different titratable sites; this makes it difficult to identify PT pathways and to characterize the mechanisms of PT reactions.

This is the area where dynamic simulations of explicit proton-transfer reactions come into play. Tuckerman et al. studied the shared proton in hydrogen bonds[18] and a hydrated excess proton in water[19] using the Car–Parrinello molecular dynamics (CPMD) method.[20,21] Lobaugh and Voth investigated proton transport in water by simulating an excess proton in a box of water molecules[22] within the centroid molecular dynamics[23] framework and by using a multistate empirical valence bond (MS-EVB) model for proton transfer.[24–26] A recent study also presented the dynamic simulation of pK_a values for amino acid side-chain analogues[27] using the MS-EVB model and the umbrella sampling technique.[28,29] The deviation between their computed value and the experimental pK_a value was 1–2 pK_a units. CPMD combined with metadynamics and transition-path sampling was employed to compute free-energy profiles for the deprotonation of acetic acid in water.[30] Several further applications showed the importance and success of studying PT in protein systems by theoretical approaches, for instance, PT in bacteriorhodopsin,[31] PT in gramicidin A,[32,33] PT along a water chain in the D pathway of COX,[34] and proton translocation in carbonic anhydrase.[35]

A simulation model of intermediate accuracy, the Q-HOP MD method, was introduced by our research group in 2001 to study dynamic proton transport between general titratable sites in biomolecular systems.[36–39] In the Q-HOP scheme, the PT probabilities for each proton-donor and -acceptor pair are calculated using a semiempirical approach during the MD simulation (see the Supporting Information for details). Depending on whether PT occurs (by comparing the PT probability to a random number), the topology of the system is modified or kept unchanged before the next step of MD simulation. The transfer probabilities depend on the momentary donor–acceptor distance (R_{DA}) and the energy difference between the minima at the donor and acceptor (E_{12}). This method has been applied successfully to study the proton shuttle in green-fluorescent protein[40] and to understand the mechanism of proton blockage in aquaporin.[41]

Herein we present the application of Q-HOP-MD to study the explicit protonation equilibrium of solvated acetic acid on a time scale of 50 nanoseconds and at a reasonable pH (pH 1). The pK_a of acetic acid is calculated based on the relative populations of protonated and deprotonated states observed during a 50-ns-long Q-HOP MD simulation. By analyzing the unbiased MD simulation, we can also identify the proton-hopping mechanism and the driving force of the activated processes of proton transfer. This study thus serves as a proof of principle of the method, and it provides detailed mechanistic insight into atomistic protonation equilibria on two separate time scales, femtoseconds and nanoseconds.

During the Q-HOP MD simulation, two types of protonation equilibria were observed. Figure 1 a,b shows the position of the "free" proton and the distance between the hydronium ion and the deprotonated acetic acid (when the proton stays on hydronium ion) during the first 10 ns. (The results for the full length of the simulation are presented in Figure 5 of the Supporting Information.) Two different situations can be distinguished. The first type of protonation equilibrium, "proton swapping", involves only the acetic acid and a nearby H_2O/H_3O^+ molecule, which forms a hydrogen bond with acetic acid. The other type of protonation

[*] W. Gu, Dr. T. Frigato, Prof. Dr. V. Helms
Zentrum für Bioinformatik
Universität des Saarlandes
66041 Saarbrücken (Germany)
Fax: (+49) 681-302-64180
E-mail: volkhard.helms@bioinformatik.uni-saarland.de
Homepage: http://gepard.bioinformatik.uni-saarland.de
Dr. T. P. Straatsma
Computational Sciences and Mathematics Division
Pacific Northwest National Laboratory
Richland, WA 99352 (USA)

[**] NWchem Version 4.7, as developed and distributed by the Pacific Northwest National Laboratory (PNNL). P.O. Box 999, Richland, WA 99352 (USA), and funded by the US Department of Energy, was used for the calculation. We thank Elena Herzog from MPI Frankfurt for computation of the *cis* conformation of acetic acid. We thank Dr. Michael Hutter and Dr. Tihamér Geyer for valuable discussion. We thank the EMSL Grand Challenge Project (project gc3551) from PNNL for providing the computing resources.

Supporting information for this article is available on the WWW under http://www.angewandte.org or from the author.

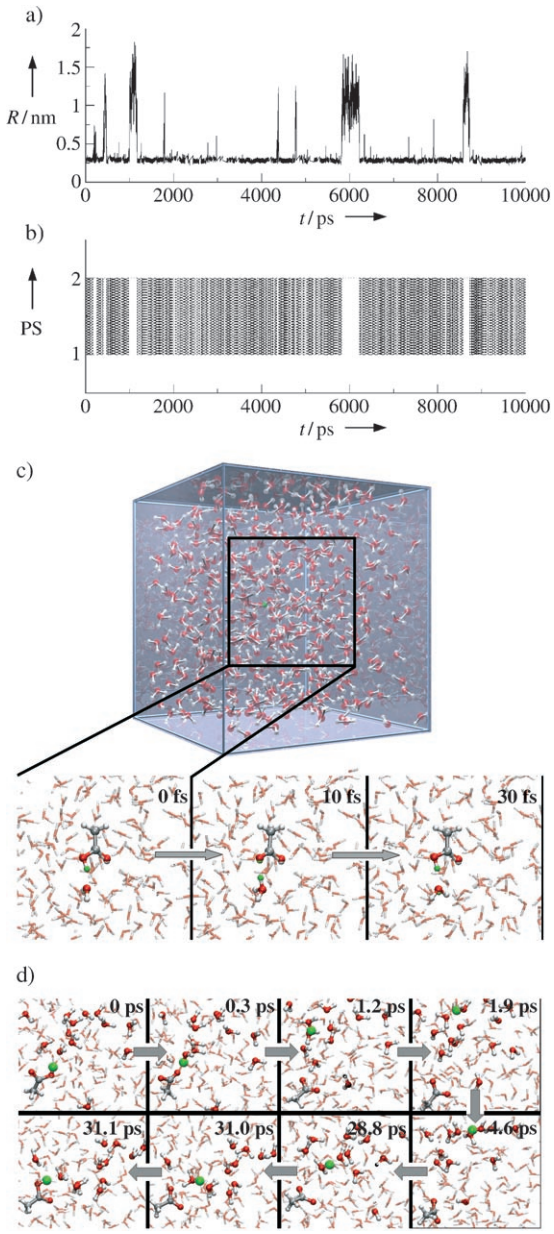

Figure 1. a) Time evolution of the distance (R) between the O_δ atom of acetic acid and the O atom of H_3O^+. b) Time evolution of the protonation states (PS) of the system: 1 denotes the state in which the proton is located on the acetic acid, 2 denotes the state in which the proton is bound to H_3O^+. c) Snapshots of a "fast-swapping" phase (the simulation box is shown at the top and the donor–acceptor pair is enlarged). d) Snapshots of a typical traveling phase lasting 31 ps and involving 16 different water molecules. Only the first four and the last three transfer steps and the molecules involved are shown; oxygen atoms are red, and protons that are transferred are green.

equilibrium, "traveling proton", involves an excess proton and all water molecules of the simulation box (see Figure 1c,d).

The first scenario accounts for more than 90% of the total PT events (Figure 1b). Although the proton is energetically more favorable on acetic acid, it may frequently "visit" the bound water molecule driven by environmental fluctuations (see below). In most cases, it will almost immediately hop back to acetic acid. During this fast proton swapping, the population of protonated acetic acid is much higher (97%) than the population of hydronium ions. This is in keeping with the fact that protonated acetic acid is energetically more favorable than the hydronium ion. These observations are in excellent agreement with those of Park et al.[30]

In some cases of fast proton swapping, the proton does not hop back to acetic acid but escapes to another water molecule hydrogen-bonded to the hydronium ion. This process may continue, and the proton starts "traveling" in the water box (see the peaks in Figure 1a). Such traveling periods last from a few picoseconds to hundreds of picoseconds before the proton eventually hops back to the acetic acid. They were observed several times every nanosecond. The total time spent with traveling amounts to slightly less than 7% of the total simulation time. Although we did not test this so far, for larger boxes it seems very plausible that the duration of the traveling events depends on the size of the simulation box in a proportional manner. Figure 1c,d illustrate characteristic snapshots of both scenarios.

Figure 2 shows the radial distribution of hydronium ions around the two carboxyl oxygen atoms of the acetic acid. The first dominant peak at 2.4–2.6 Å is due to the fast proton

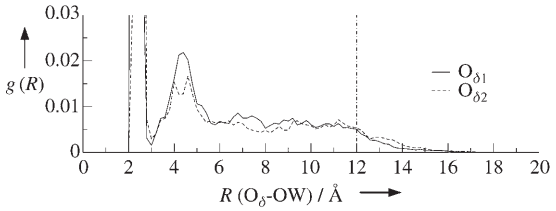

Figure 2. Radial distribution (normalized) of hydronium ions around the two carboxyl oxygen atoms of the acetic acid. (Complete plot is shown in the Supporting Information.)

swapping between the acetic acid and bound water molecules mentioned above. A small second peak appears at 4–5 Å, which belongs to the first solvation shell of the AcA^-–H_3O^+ pair. The distribution function then becomes flat between 5 Å and 12 Å, and drops slowly to 0 for even longer distances. The flat distribution indicates that the hydronium ion is uniformly distributed when the proton is traveling in the simulation box, and allows us to estimate the traveling time of the proton for box sizes much larger than 5 Å (where the second peak ends). The drop of the distribution function beyond 12 Å results from the corner effects of the cubic box with 24-Å dimensions. The dashed and solid lines show the radial distributions separately computed for both carboxylic oxygen atoms of acetic acid. The difference between the two lines gives an indication of the statistical error of the simulation.

Figure 3a shows a typical scenario for proton transfer between acetic acid and H_3O^+/H_2O. To understand the mechanism of the proton hopping, we examined the hydrogen-bonding network of a subsystem consisting of the donor–acceptor pair and three water molecules that form hydrogen bonds with either the donor or the acceptor atom. Here, Wat1 and Wat2 denote the two closest water molecules that form hydrogen bonds (as acceptors) with the hydronium ion, and

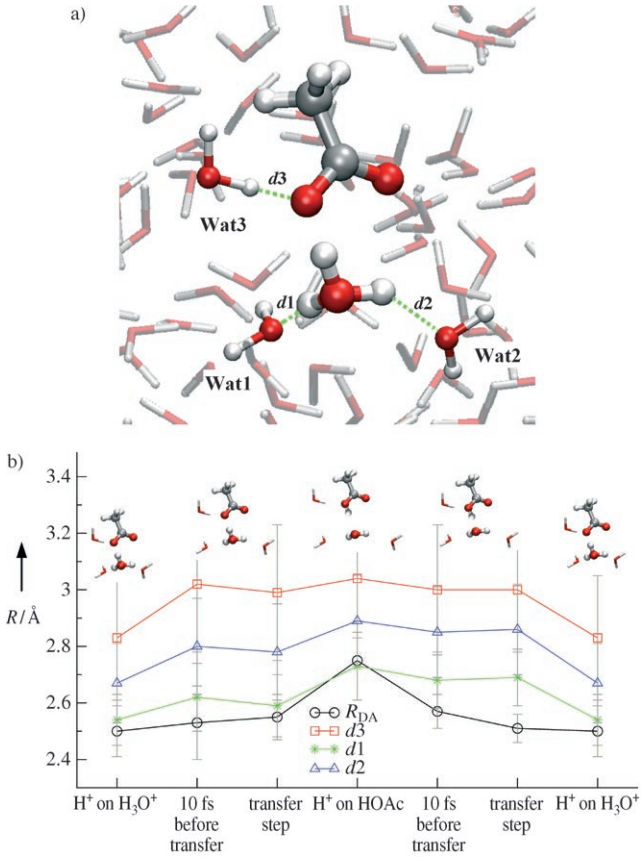

Figure 3. a) A snapshot of a typical transfer scenario observed during the simulation. The donor (H_3O^+) and the acceptor (AcOH) as well as the three closest water molecules are shown using the "atom and bond" representation. O red, H white. The green dashed lines represent possible hydrogen bonds. b) Evolution of the distances R_{DA} and *d*1–*d*3. R_{DA}: O_δ–OW(H_3O^+), *d*1: OW(H_3O^+)–OW1, *d*2: OW-(H_3O^+)–OW2, *d*3: O_δ–OW3.

Wat3 denotes the closest water molecule that forms a hydrogen bond (as donor) with the O_δ atom of acetic acid. Figure 3b displays the average distances between the hydrogen-bonding atoms in different protonation states as well as conformations right before the proton hopping. The three distances between OW atoms of water molecules Wat1–Wat3 and their hydrogen-bonding partners are labeled *d*1–*d*3, respectively. R_{DA} denotes the distance between the donor and acceptor atoms.

We start the discussion from the left side in an arrangement in which the proton resides on the hydronium ion, and the three water molecules Wat1–Wat3 are located very close to their hydrogen-bonding partners [*d*1: (2.54 ± 0.09) Å; *d*2: (2.67 ± 0.14) Å; *d*3: (2.83 ± 0.22) Å]. Also the donor and acceptor atoms are very close to each other [R_{DA}: 2.50 ± 0.09) Å]. These close contacts stabilize the charge-separated state of the system. At the time intervals 10 fs before and at the time of proton transfer to the acetic acid, all three water molecules are displaced from the donor–acceptor pair [*d*1: (2.62 ± 0.12) Å (10 fs before transfer), (2.59 ± 0.11) Å (at transfer step); *d*2: (2.80 ± 0.17), (2.78 ± 0.17) Å; *d*3: (3.02 ± 0.24), (3.00 ± 0.25) Å]. At this stage, the donor and the acceptor atoms are also slightly more separated [R_{DA}: (2.53 ± 0.13), (2.55 ± 0.08) Å]. This concerted movement destabilizes the actual protonation state, and the proton hopping is facilitated. After the proton is transferred to the acetic acid, the environment quickly adapts to the new protonation state [*d*1: (2.73 ± 0.12) Å; *d*2: (2.89 ± 0.16) Å; *d*3: (3.04 ± 0.24) Å]. One pronounced change is the significantly extended distance between donor and acceptor: R_{DA} increases from (2.55 ± 0.08) to (2.75 ± 0.14) Å. Considering the back transfer from acetic acid to water, the main driving force seems again a strong decrease of R_{DA} accompanied by small decreases of the distances between water molecules. These results are very similar to those of Park et al.,[30] who observed the formation of contact ion pairs after rearrangement of the solvent molecules.

As mentioned before, acetic acid was protonated during about 90% of the total simulation. For the current simulation setup, the concentration of the free proton (H_3O^+) is 0.1 mol L^{-1} when the proton stays on the hydronium ion and 0 when it stays on the acetic acid. Following the classical definition of pK_a [Eq. (1)], the pK_a value of acetic acid

$$pK_a = \log \frac{[H^+][A^-]}{[HA]} \qquad (1)$$

estimated from the observed populations in our simulation is about 3.0. By dividing the entire trajectory into 25 windows (2-ns each), we derive an average relative population of AcOH of 0.90 ± 0.09 (see the Supporting Information). This corresponds to pK_a values from 2.4 to 4.5. For comparison, the experimental pK_a of acetic acid is 4.7. Since we didn't tune any simulation parameters to reproduce the experimental pK_a value, we consider the computed pK_a a very acceptable value.

Certainly, other computational techniques allow computing the average pK_a much more precisely at a much lower computational cost.[14,16,17] However, besides the pK_a value, the Q-HOP concept also provides insights into time-dependent processes and identifies the driving forces of the activated processes of proton transfer. Moreover, one can obtain an idea of possible mechanistic PT pathways. If desired, individual cases along the discovered pathways can then be studied at much higher accuracy using electronic structure theory coupled to rate theories such as variational transition state theory (VTST).[42]

Another possible comparison between our simulation and experimental observation is the diffusion coefficient of the excess proton. Our calculated result [$(9.29 \pm 1.43) \times 10^{-1}$ Å^2 ps^{-1}] nicely agrees with the experimental value of 9.3×10^{-1} Å^2 ps^{-1}. Slightly different results between 9.0×10^{-1} and 9.5×10^{-1} Å^2 ps^{-1} are obtained for windows of different sizes (see the Supporting Information), which shows that the value is essentially independent of the size of the windows. This good agreement indicates that the Q-HOP MD simulation correctly characterizes the diffusive dynamics of the excess proton.

The main objective of this study was to show that current simulation methodology allows the simulation of the dynamic protonation equilibrium between an amino acid side-chain analogue and the surrounding bulk water. In contrast to previous studies,[27,30] it was not necessary to impose a certain

PT pathway in our simulation. Instead, the pathway and the driving forces are revealed by the simulations. Therefore, one can easily extend the current simulation methodology to protein or polymer systems, where the proton travels over large distances and the PT pathway is not known beforehand.

The changes of $d1$–$d3$ in different protonation states of the system (Figure 3b) as well as the dynamic evolution of $d1$–$d3$ in the two types of protonation equilibria (see Figure 7a in the Supporting Information) indicate that the fluctuations of the hydrogen-bonding network involving the donor–acceptor pair are important driving forces for the activation of the PT process. Another important criterion for hopping is the distance between donor and acceptor, R_{DA}. The hopping events happen only when R_{DA} and $d1$–$d3$ fulfil certain requirements. In vacuum, protonated acetic acid is energetically more favorable than the hydronium ion at large R_{DA} values. At decreasing R_{DA} values, the protonated acetic acid becomes less favorable. In an aqueous solution environment, the well-established hydrogen-bonding network with neighboring water molecules provides further stabilization of the hydronium ion and PT may occur. Fluctuations of this hydrogen-bonding network, however, weaken this effect and facilitate the back transfer of the proton to acetic acid.

In previous theoretical studies on the hydrated excess proton in water[19,43] the mechanism of proton hopping between closest water molecules was proposed as the fluctuation-induced breakage of a hydrogen bond between the first and second solvation shell of the hydronium ion.[19] The fluctuation of the hydrogen-bonding network in some stages destabilizes the donor (H_3O+) and stabilizes the protonated acceptor, which results in the PT events.[43] The transfer statistics observed in our simulation agree well with this mechanism. Moreover, the changes of R_{DA} in our simulation may also be coupled to the fluctuations of the hydrogen-bonding network.

In conclusion, the dynamic protonation equilibrium between an amino acid side-chain analogue and bulk water was successfully observed for the first time through unbiased computer simulations. Two different types of proton transfer were identified during a 50-ns Q-HOP MD simulation. During the fast-swapping equilibrium that occupied most of the simulation time, the proton mostly stayed on the acetic acid. Several times per nanosecond the proton left the acetic acid, was then exchanged between different water molecules, and finally came back to the acetic acid. The fluctuations of the hydrogen-bonding network as well as the donor–acceptor distance were found to be the driving forces of the activated processes. The pK_a of acetic acid calculated based on the relative population of protonated and deprotonated states and the diffusion coefficient of the excess proton agree well with the experimental measurements. Since the computational cost of the Q-HOP method is comparable to that of classical MD simulations, simulations on this time scale are feasible for many applications on organic and biomolecular systems as well as in polymer science.

Experimental Section

The segments of protonated and deprotonated acetic acid were constructed based on the segments of protonated and deprotonated aspartic acid in the AMBER force field.[44] The C_α–C_β bond was deleted, and the C_α atom was replaced by an H_β atom. All bonded and non-bonded parameters of the newly added H_β atom were set to the same values as those of the other two H_β atoms. The remaining partial atomic charge was added to the C_β atom to make the net charge of the segment integer (0 for protonated acetic acid and −1 for deprotonated acetic acid). The AMBER and the Q-HOP parameterization of acetic acid used in this study is listed in detail in the Supporting Information.[45]

The Q-HOP MD simulations as well as the single-point calculations for charge fitting were performed using a modified version of the NWChem 4.7 package employing the AMBER99 force field.[44] In this implementation, the Particle Mesh Ewald (PME) method[46] is used for calculating long-range electrostatic interactions during molecular dynamics. For evaluating the environmental correction of E_{12}^{env} (see the Supporting Information), all coulombic interactions were computed between the donor–acceptor pairs and the other atoms of the simulation box. Periodic images were translated so that the donor–acceptor atoms are always in the center of the box. In the Q-HOP MD simulations, the $AcOH/H_2O$ pair and the AcO^-/H_3O^+ pair (same as in the MD simulation for generating favorable hopping geometries) were each solvated in cubic boxes of 24-Å side length, using SPC/E water molecules.[47] All coordinate sets were first subjected to 500 steps of steepest-descent energy minimization (Q-HOP switched off). The solvent and modeled residues were then relaxed during a 100-ps MD simulation at 300 K prior to the Q-HOP MD simulation. Then two 10-ns Q-HOP MD simulations were performed on each system. When the two simulations gave very similar results, one simulation with AcO^-/H_3O^+ as the starting pair was extended to 50 ns. All analyses shown here are based on this 50-ns simulation. During the simulation, temperature (300 K) and pressure (1 atm) were maintained by weak coupling to an external bath.[48] The SHAKE procedure[49] was applied to constrain all bonds that contain hydrogen atoms. Non-bonded interactions were treated using a cutoff of 10 Å, and long-range electrostatic interactions were computed using the PME method as mentioned before. The time step of the simulations was 1 fs throughout. Scanning for possible PT events was performed every 10 steps, and snapshots were also recorded every 10 steps to track all hopping events. All water molecules as well as the acetic acid were treated as possible donor/acceptors. All protons of the water molecules were transferable.

The trajectory containing the traveling hydronium ion (excluding period of fast swapping) was divided into 11 parts (large windows) that are each 200-ps long. Then a sliding window of 10 ps was used to calculate the displacement of the excess proton for each large window. The diffusion constant was then computed using the Einstein relation [Eq. (2)], where the averaging was performed within a large window.

$$\langle D = \frac{|r(t)-r(0)|^2}{6t} \rangle \qquad (2)$$

Received: September 1, 2006
Revised: January 8, 2007
Published online: March 15, 2007

Keywords: acidity · carboxylic acids · molecular dynamics · proton transfer · reaction mechanisms

[1] A. Warshel, G. Narayszabo, F. Sussman, J. K. Hwang, *Biochemistry* **1989**, *28*, 3629.

[2] G. S. Li, B. Maigret, D. Rinaldi, M. F. Ruiz-Lopez, *J. Comput. Chem.* **1998**, *19*, 1675.
[3] H. Umeyama, S. Hirono, S. Nakagawa, *Proc. Natl. Acad. Sci. USA* **1984**, *81*, 6266.
[4] D. S. Lu, G. A. Voth, *J. Am. Chem. Soc.* **1998**, *120*, 4006.
[5] H. Luecke, B. Schobert, H. T. Richter, J. P. Cartailler, J. K. Lanyi, *Science* **1999**, *286*, 255.
[6] S. Iwata, C. Ostermeier, B. Ludwig, H. Michel, *Nature* **1995**, *376*, 660.
[7] H. Michel, *Biochemistry* **1999**, *38*, 15129.
[8] J. P. Abrahams, A. G. W. Leslie, R. Lutter, J. E. Walker, *Nature* **1994**, *370*, 621.
[9] S. S. Jang, S. T. Lin, T. Cagin, V. Molinero, W. A. Goddard, *J. Phys. Chem. B* **2005**, *109*, 10154.
[10] U. Borjesson, P. H. Hunenberger, *J. Chem. Phys.* **2001**, *114*, 9706.
[11] R. Burgi, P. A. Kollman, W. F. van Gunsteren, *Proteins Struct. Funct. Genet.* **2002**, *47*, 469.
[12] A. M. Baptista, P. J. Martel, S. B. Petersen, *Proteins Struct. Funct. Genet.* **1997**, *27*, 523.
[13] A. Onufriev, D. A. Case, G. M. Ullmann, *Biochemistry* **2001**, *40*, 3413.
[14] J. Mongan, D. A. Case, J. A. McCammon, *J. Comput. Chem.* **2004**, *25*, 2038.
[15] M. S. Lee, F. R. Salsbury, C. L. Brooks, *Proteins Struct. Funct. Bioinf.* **2004**, *56*, 738.
[16] A. M. Walczak, J. M. Antosiewicz, *Phys. Rev. E* **2002**, *66*, 051911.
[17] A. M. Baptista, V. H. Teixeira, C. M. Soares, *J. Chem. Phys.* **2002**, *117*, 4184.
[18] M. E. Tuckerman, D. Marx, M. L. Klein, M. Parrinello, *Science* **1997**, *275*, 817.
[19] D. Marx, M. E. Tuckerman, J. Hutter, M. Parrinello, *Nature* **1999**, *397*, 601.
[20] D. Marx, M. Parrinello, *J. Chem. Phys.* **1996**, *104*, 4077.
[21] M. E. Tuckerman, D. Marx, M. L. Klein, M. Parrinello, *J. Chem. Phys.* **1996**, *104*, 5579.
[22] J. Lobaugh, G. A. Voth, *J. Chem. Phys.* **1996**, *104*, 2056.
[23] J. S. Cao, G. A. Voth, *J. Chem. Phys.* **1994**, *100*, 5093.
[24] U. W. Schmitt, G. A. Voth, *J. Phys. Chem. B* **1998**, *102*, 5547.
[25] U. W. Schmitt, G. A. Voth, *J. Chem. Phys.* **1999**, *111*, 9361.
[26] T. J. F. Day, A. V. Soudackov, M. Cuma, U. W. Schmitt, G. A. Voth, *J. Chem. Phys.* **2002**, *117*, 5839.
[27] C. M. Maupin, K. F. Wong, A. V. Soudackov, S. Kim, G. A. Voth, *J. Phys. Chem. A* **2006**, *110*, 631.
[28] C. Pangali, M. Rao, B. J. Berne, *J. Chem. Phys.* **1979**, *71*, 2975.
[29] G. N. Patey, J. P. Valleau, *J. Chem. Phys.* **1975**, *63*, 2334.
[30] J. M. Park, A. Laio, M. Iannuzzi, M. Parrinello, *J. Am. Chem. Soc.* **2006**, *128*, 11318.
[31] A. N. Bondar, M. Elstner, S. Suhai, J. C. Smith, S. Fischer, *Structure* **2004**, *12*, 1281.
[32] R. Pomes, B. Roux, *Biophys. J.* **1996**, *71*, 19.
[33] R. Pomes, B. Roux, *Biophys. J.* **1998**, *75*, 33.
[34] J. C. Xu, G. A. Voth, *Proc. Natl. Acad. Sci. USA* **2005**, *102*, 6795.
[35] S. Braun-Sand, M. Strajbl, A. Warshel, *BioPhys. J.* **2004**, *87*, 2221.
[36] M. A. Lill, V. Helms, *J. Chem. Phys.* **2001**, *115*, 7985.
[37] M. A. Lill, V. Helms, *J. Chem. Phys.* **2001**, *115*, 7993.
[38] M. A. Lill, V. Helms, *J. Chem. Phys.* **2001**, *114*, 1125.
[39] M. A. Lill, M. C. Hutter, V. Helms, *J. Phys. Chem. A* **2000**, *104*, 8283.
[40] M. A. Lill, V. Helms, *Proc. Natl. Acad. Sci. USA* **2002**, *99*, 2778.
[41] B. L. de Groot, T. Frigato, V. Helms, H. Grubmüller, *J. Mol. Biol.* **2003**, *333*, 279.
[42] A. D. Isaacson, D. G. Truhlar, *J. Chem. Phys.* **1982**, *76*, 1380.
[43] H. Lapid, N. Agmon, M. K. Petersen, G. A. Voth, *J. Chem. Phys.* **2005**, *122*, 014506.
[44] W. D. Cornell, P. Cieplak, C. I. Bayly, I. R. Gould, K. M. Merz, D. M. Ferguson, D. C. Spellmeyer, T. Fox, J. W. Caldwell, P. A. Kollman, *J. Am. Chem. Soc.* **1996**, *118*, 2309.
[45] E. Herzog, T. Frigato, V. Helms, C. R. D. Lancaster, *J. Comput. Chem.* **2006**, *27*, 1534.
[46] U. Essmann, L. Perera, M. L. Berkowitz, T. Darden, H. Lee, L. G. Pedersen, *J. Chem. Phys.* **1995**, *103*, 8577.
[47] H. J. C. Berendsen, J. R. Gigera, T. P. Straatsma, *J. Phys. Chem.* **1987**, *91*, 6269.
[48] H. J. C. Berendsen, J. P. M. Postma, W. F. van Gunsteren, A. DiNola, J. R. Haak, *J. Chem. Phys.* **1984**, *81*, 3684.
[49] J. P. Ryckaert, G. Ciccotti, H. J. C. Berendsen, *J. Comput. Phys.* **1977**, *23*, 327.

